

# **Enhancing the Solubility and Bio-activity of Phenolic Acids by Their Conversion into Supra-molecular Ionic Salts**

**Wang, Zhenyuan<sup>1</sup>; Wang, Mi<sup>1,3</sup>; Fan, Wenhua<sup>2</sup>; Tang, Jinshan<sup>2</sup>; Zhang, Qiqing<sup>2</sup>; Zhang, Jiaheng<sup>1,3\*</sup>**

<sup>1</sup> Shenzhen Shinesky Biological Technology Co. Ltd., Shenzhen, China; <sup>2</sup> Guangzhou Fanwenhua Cosmetic Co. Ltd., Guangzhou, China; <sup>3</sup> Sauvage Laboratory for Smart Materials, Harbin Institute of Technology (Shenzhen), Shenzhen, China

\* Zhang, Jiaheng, Shenzhen Shinesky Biological Technology Co. Ltd., Shenzhen, China, +86 0755-86574709, zhangjiaheng@hit.edu.cn

## **Abstract**

**Background:** As a prominent class of bio-active substances, phenolic acids have various bioactive properties, such as antioxidant, antibacterial and anti-inflammatory. However, the limited water solubility is a major drawback for phenolic acids to be widely used in cosmetics.

**Methods:** To enhance the water solubility and bioactivity of phenolic acids, a novel family of matrinium-based supra-molecular ionic salts, were designed and synthesized, featuring a series of phenolic acid anions derived from natural plants, i.e., Gallic acid, vanillic acid, caffeoic acid, syringic acid, etc.

**Results:** The structure of resulting supra-molecular ionic salts was confirmed by NMR spectroscopy, X-ray crystallography, infrared spectroscopy, and elemental analysis, showing a high purity level of all synthesized ionic structures. Results of the water solubility experiments showed that these new salts were significantly more soluble in water (up to 3 orders of magnitude higher) than the corresponding phenolic acids. The antioxidant properties were evaluated by using the 1,1-Diphenyl-2-picrylhydrazyl and 2,2'-azino-bis-(3-ethylbenzothiazoline)-6-sulfonic acid assays in the solutions. The IC<sub>50</sub> values of the Supra-molecular ionic salts were significantly lower than that for the phenolic acids.

**Conclusion:** When compared with their respective acidic precursors, the matrinium-based supra-molecular ionic salts display superior water solubility, antioxidant and antibacterial activities, as well as lower cytotoxicity profiles. Consequently, the bio-renewable supra-molecular phenolic compounds should have potential applications as bio-active substances for use in cosmetics, food, pharmacy, etc.

**Keywords:** bioactive, supra-molecular ionic salts, matrine, phenolic acids, water solubility.

## Introduction

It is well-known that anti-oxidation is an important strategy for aging precaution. Excess free radicals or oxidants can break down cells and tissues, affect metabolic function, and cause various health problems, such as cancer, arteriosclerosis, diabetes, cataract, cardiovascular diseases, Alzheimer's, arthritis, etc. [1]. Thus, antioxidant performance is one of the most important functional demands of healthcare and cosmetic products. An adequate intake of antioxidants is a benefit to slowing down body degradation and skin aging, resulting in a youthful look. Antioxidants can be obtained through food, but when a sub-health state occurs, additional antioxidants are required. There are mainly three types of natural antioxidants: phenols, carotenoids, and vitamins. Phenolic acids are a class of organic acids containing phenolic rings, which are relatively high in the fruits of many plants [2]. Many phenolic acids derived from plants are used in various cosmetics, as antioxidants or whitening ingredients, etc. But the poor water solubility of phenolic acids has dramatically blocked their dosage and bioavailability in cosmetics [3,4]. Although this problem can be resolved through formulation design, such as lipid encapsulation, the process is complicated with limited application scenarios [5,6].

Salt formation and co-crystallization are two important methods to improve water solubility in the pharmaceutical field, and the selection of counterions or co-formers is a key factor affecting the product performance [7,8]. There are many reports on the co-crystallization of phenolic acids to achieve better solubility and bioavailability, but relatively fewer studies on salt formation [9-11]. Matrine is an alkaloid extracted from the roots and fruits of the legume Sophora radix, which has antibacterial, anti-inflammatory, diuretic, and liver-protecting effects [12]. Moreover, matrine is also a functional cosmetic ingredient, which can relieve skin itching, balance oil, and promote the repair of damaged blood vessels, nerves, and cells. Some previous studies have shown that matrine can form salts with weak acids, and results in enhanced bioactivity of products [13-14]. Thus, salt formation with

matrine is supposed to be a feasible and effective strategy to increase the water solubility and bioactivity of phenolic acids.

In this work, a novel type of matrinium-based supra-molecular ionic salts (MSIS) were synthesized to enhance the water solubility and bioactivity of 4 kinds of phenolic acids with poor water solubilities, i.e., gallic acid (H[Gal]), vanillic acid (H[Van]), caffeic acid (H[Caf]), syringic acid (H[Syr]). The composition and structure of MSIS were characterized by nuclear magnetic resonance (NMR), Fourier transform infrared (FT-IR), X-ray diffraction, and element analysis, as well as the water solubility, antibacterial activity, antioxidant efficiency, and cytotoxicity of MSIS were analyzed and compared with those of the phenolic acids and matrine. Besides, the influence of crystal structure on the MSIS properties was also systematically studied, and a synergistic effect between the matrine cations and phenolic anions was found, resulting in enhanced water solubility, antibacterial activity, and antioxidant efficiency, and lower cytotoxicity of MSIS.

## Materials and Methods

**Materials.** Matrine (98%), H[Gal] (99%), H[Van] (98%), H[Caf] (98%), H[Syr] (98%), ascorbic acid (AA, 99%), 6-hydroxy-2,5,7,8-tetramethylchroman-2-carboxylic acid (Trolox, 98%) and K<sub>2</sub>S<sub>2</sub>O<sub>8</sub> (99.5%) were obtained from Shanghai Aladdin Biochemical Technology Co., Ltd. 1,1-Diphenyl-2-picrylhydrazyl (DPPH, 96%) and 2,2'-azino-bis-(3-ethylbenzothiazoline)-6-sulfonic acid (ABTS, 98%) were purchased from Sinopharm Chemical Reagent Co., Ltd., China). 3-(4,5-dimethyl-2-thiazolyl)-2,5-diphenyl-2-H-tetrazolium bromide (MTT) were acquired from Sigma Aldrich, Shanghai, China. Normal human epidermal keratinocytes (NHEK) and the special culture medium for keratinocytes (KC2500) were provided by Guangdong Biocell Biotechnology Co., Ltd. *Escherichia coli* (*E. coli*, 8099) and *Staphylococcus aureus* (*S. aureus*, ATCC6538) bought from China Center of Industrial Culture Collection (CICC). Mueller-Hinton Broth (MHB) was acquired from Qingdao Hope Bio-Technology Co., Ltd.

**Synthesis.** 4 types of MSIS, i.e., matrinium gallate ([Mat][Gal]), matrinium vanillate ([Mat][Van]), matrinium caffeinate ([Mat][Caf]) and matrinium syringate ([Mat][Syr]), were synthesized by a simple neutralization reaction between matrine and their respective phenolic acids, i.e., gallic acid (H[Gal]), vanillic acid (H[Van]), caffeic acid (H[Caf]) and syringic

acid (H[Syr]). In brief, a phenolic acid was dissolved in ethanol, and equimolar matrine was added to the solution several times; after reaction at 60 °C for 24 h under a nitrogen atmosphere, the product was concentrated, crystallized, filtered, and washed with cold ethanol for 3 times; finally, the MSIS was obtained by vacuum drying. Besides, single crystals of [Mat][Gal] and [Mat][Syr]·CH<sub>3</sub>OH were prepared by recrystallizing the MSIS from methanol solutions, while single crystals of [Mat][Van]·H<sub>2</sub>O and [Mat][Caf]·H<sub>2</sub>O were recrystallized from aqueous solutions.

**General characterization.** The composition and structure of MSIS were analyzed using NMR spectroscopy from a Bruker Avance 400 MHz spectrometer (Billerica, MA, USA), FT-IR spectroscopy from a Perkin Elmer Frontier spectrometer (Bruker, Waltham, MA, USA), X-ray diffraction data from an Agilent SuperNova single-crystal diffractometer (Bruker, Billerica, MA, USA) and elemental analysis from a Flash EA-1112 elemental analyzer (Thermo, Waltham, MA, USA).

**Water solubility.** The water solubilities of matrine, phenolic acids, and MSIS were determined by the typical shake-flask method. Firstly, the calibration curve of each sample was drawn between the concentration and its absorbance at the maximum absorption wavelength, with the assistance of a UV-vis spectrophotometer (PerkinElmer Lambda 365, Waltham, MA, USA). Then, a supersaturated solution of each sample was prepared by mixing the solid with inadequate amount of deionized water. After equilibration, the saturated supernatant was collected by filtration with a syringe filter (0.22 µm pore size). Finally, the saturated supernatant was diluted with deionized water to an appropriate absorbance, and the water solubility of each sample was calculated referring to its calibration curve.

**Antibacterial activity.** The antibacterial activities of matrine, phenolic acids, and MSIS were determined by the broth microdilution method referring to previous work with some modifications [22]. *E. coli* and *S. aureus* were tested as typical examples of gram-negative and positive bacteria, respectively. Firstly, one type of bacteria was incubated in MHB medium to the logarithmic phase with a concentration of 1×10<sup>7</sup> CFU/mL. Then, 180 uL of the sample solution was added into a well of the 96-well plate and serially diluted to a series of concentrations. Subsequently, 20 uL/well of the bacteria suspension was mixed with the

sample solution, while pure medium and pure bacteria suspension were added as NC and PC groups. After incubation at 37 °C for 24h, OD at 600 nm was recorded to investigate the bacterial growth. Finally, the antibacterial activity was represented by the minimal inhibitory concentration (MIC), which is the lowest sample concentration to completely inhibit bacterial growth.

**Antioxidant assay.** The antioxidant ability of matrine, phenolic acids, and MSIS were determined by the DPPH and ABTS methods, which are very popular in vitro antioxidant assays. The DPPH radical scavenging assay was conducted following a previous work with some modifications [23]. Firstly, each sample was dissolved in 80% (v/v in water) ethanol to obtain the tested solution with various concentrations. Then, 180 µL/well of ethanol solution containing 0.2 mM DPPH was added to a 96-well microplate and mixed with 20 µL/well of the tested solution, which was substituted by 20 µL of 80% ethanol and 20 µL of AA solution for NC and PC, respectively. After 30 min of incubation at 25 °C in darkness, the absorbance of each well at 515 nm was recorded, and the DPPH radical scavenging ratio was calculated according to the following equation:

$$\text{Scavenging Ratio (\%)} = [(A_c - A_s) / A_c] \times 100\% \quad (2)$$

where  $A_s$  and  $A_c$  are the absorbance values of the wells treated with the tested samples and NC, respectively. Finally, the DPPH radical scavenging ability of each sample was represented by  $IC_{50}$ , which is the concentration with 50% scavenging of DPPH radicals and estimated by GraphPad Prism 8.

The ABTS radical scavenging assay was carried out following a previous study with minor modifications [24]. Firstly, the aqueous solution containing 7 mM ABTS was mixed with the same amount of aqueous solution containing 2.45 mM  $K_2S_2O_8$ , and reacted for 14 h at 25 °C in darkness to obtain radicals. Then, the working solution with an appropriate absorbance ( $0.70 \pm 0.02$ ) at 734 nm was prepared by diluting the above mixture with 80% ethanol. After that, 200 µL/well of ABTS working solution was added to a 96-well microplate and mixed with 10 µL/well aqueous solution containing various concentrations of the tested sample, which was substituted by 80% ethanol and Trolox solution for NC and PC, respectively. Subsequently, the mixture solutions were incubated at 25 °C in darkness for 6

min, and their absorbance at 734 nm was characterized. Finally, the IC<sub>50</sub> values were also estimated by GraphPad Prism 8 to represent ABTS radical scavenging ability.

**Cytotoxicity.** NHEK cells were cultured in KC2500 medium and seeded into 96-well plates at a density of 1×10<sup>4</sup> cells/well. After 24 h of incubation at 37 °C with an atmosphere of 5% CO<sub>2</sub> and relative humidity of 95%, each well was added with 200 μL of medium containing various concentrations of the tested samples. For the samples with water solubility below 10 mg/mL, 0.5% (v/v) of DMSO was adopted to ensure complete dissolution. Besides, pure medium without cells, cells treated with pure medium, and cells treated with 10% DMSO were also tested as blank (BC), negative (NC), and positive controls (PC), respectively. After another incubation of 24 h, the supernatant was discarded, followed by the addition of 10 μL/well of 5 mg/mL MTT. Subsequently, with an additional incubation of 4 h, the supernatant was removed and 150 μL/well of DMSO was added to dissolve the cells. Finally, the optical density (*OD*) at 490 nm was recorded on a Bio-Tek Gen5 microplate reader (Winooski, VT, USA), and the cell viability was calculated according to the following equation:

$$\text{Cell viability (\%)} = (OD_s - OD_{BC})/(OD_{NC} - OD_{BC}) \times 100\% \quad (1)$$

where *OD<sub>s</sub>*, *OD<sub>BC</sub>*, and *OD<sub>NC</sub>* are the *OD* values of the wells treated with the tested samples, BC and NC, respectively. The cytotoxicity of each sample was represented by IC<sub>50</sub>, which is the concentration with 50% inhibition of cell viability and estimated by GraphPad Prism 8.

**Statistical analysis.** The above measurements of water solubility, cytotoxicity, DPPH assay, ABTS assay, and antibacterial ability were performed in triplicate, and the results were expressed as the mean ± standard deviation. Two groups of data were compared by the T-test, and a significant difference was regarded as p < 0.05.

## Results and Discussion

The <sup>1</sup>H and <sup>13</sup>C NMR spectra of MSIS were recorded in MeOD, and the results (Fig.1) are the same as the mixture of their respective raw materials. Taking [Mat][Gal] as an example, its <sup>1</sup>H and <sup>13</sup>C NMR spectra were identical to the mixture of matrine and H[Gal].

This means that no side reactions occurred except for the acid-base neutralization. The FT-IR spectra of matrine and MSIS were measured, while the FT-IR spectra of H[Gal], H[Van], H[Caf], H[Syr] were obtained from the SDBS spectral database ([http://sdbs.db.aist.go.jp/sdbs/cgi-bin/direct\\_frame\\_top.cgi](http://sdbs.db.aist.go.jp/sdbs/cgi-bin/direct_frame_top.cgi)). The FT-IR spectrum of matrine mainly contains peaks at 2927, 2734, 1641, 1622, 1467, 1415, 1339, 1280, 1254, 1195, 1168, 1128, 1091, 1066, 1022, 989, 918, 854, 648, 456 cm<sup>-1</sup>. The peaks at 3000 – 2600 cm<sup>-1</sup> and 1600-1650 cm<sup>-1</sup> refer to the C-H stretching of alkane groups and C=O stretching of amide groups. The FT-IR spectrum of H[Gal] mainly contains peaks at 3286, 3044, 1703, 1618, 1551, 1544, 1469, 1450, 1341, 1309, 1266, 1257, 1248, 1028, 859, 704 cm<sup>-1</sup>. The peaks at 3000 – 2600 cm<sup>-1</sup> and 1600-1650 cm<sup>-1</sup> refer to the C-H stretching of alkane groups and C=O stretching of amide groups. The wide peak at 3500 – 3000 cm<sup>-1</sup> refers to the combination of O-H stretching of carboxyl and phenolic hydroxyl groups, while the peaks at 1750 – 1600 cm<sup>-1</sup> and 1600 – 1500 cm<sup>-1</sup> refer to the asymmetric stretching and O-H bending of carboxyl groups, respectively. As it is shown in Fig.2a, the wide peak at 3500 – 3000 cm<sup>-1</sup> of H[Gal] disappeared and a new wide peak at 3000 – 2500 cm<sup>-1</sup> appeared for [Mat][Gal], indicating the decrease of O-H bonds and the appearance of N<sup>+</sup>-H bonds [15-17]. Meanwhile, the O-H bending peak of the H[Gal] carboxyl groups disappeared and the asymmetric stretching peaks moved to 1650 – 1500 cm<sup>-1</sup>, indicating the proton transfer between H[Gal] and matrine [18,19], and the strong static interaction between the matrinium cations and gallate anions.

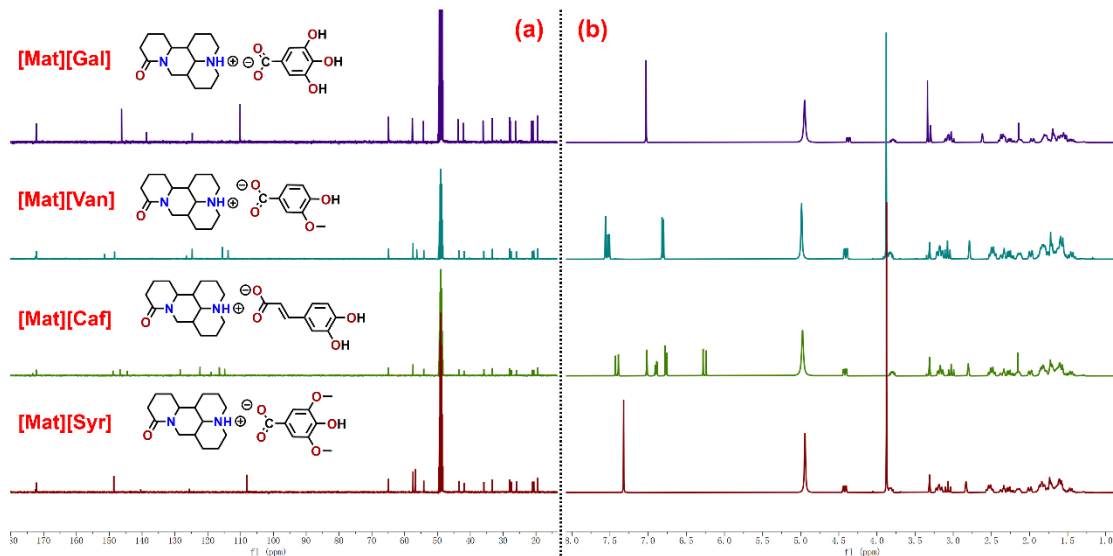


**Fig.1** The (a) <sup>13</sup>C and (b) <sup>1</sup>H NMR spectra of MSIS.

The FT-IR spectrum of H[Van] mainly contains peaks at 3486, 2990, 2650, 1686, 1599, 1525, 1438, 1306, 1241, 1207, 1114, 1030, 765 cm<sup>-1</sup>. The sharp O-H stretching peak at 3486 cm<sup>-1</sup> was attributed to the strong hydrogen-bond intra-molecules, which also appeared in the FT-IR spectra of H[Caf] and H[Syr]. Similar to that of [Mat][Gal], the wide peak corresponding to the combination of O-H stretching of carboxyl and phenolic hydroxyl groups disappeared, and the wide peak corresponding to the N<sup>+</sup>-H stretching vibrations appeared, indicating a proton transfer also occurred in [Mat][Van], [Mat][Caf] and [Mat][Syr].

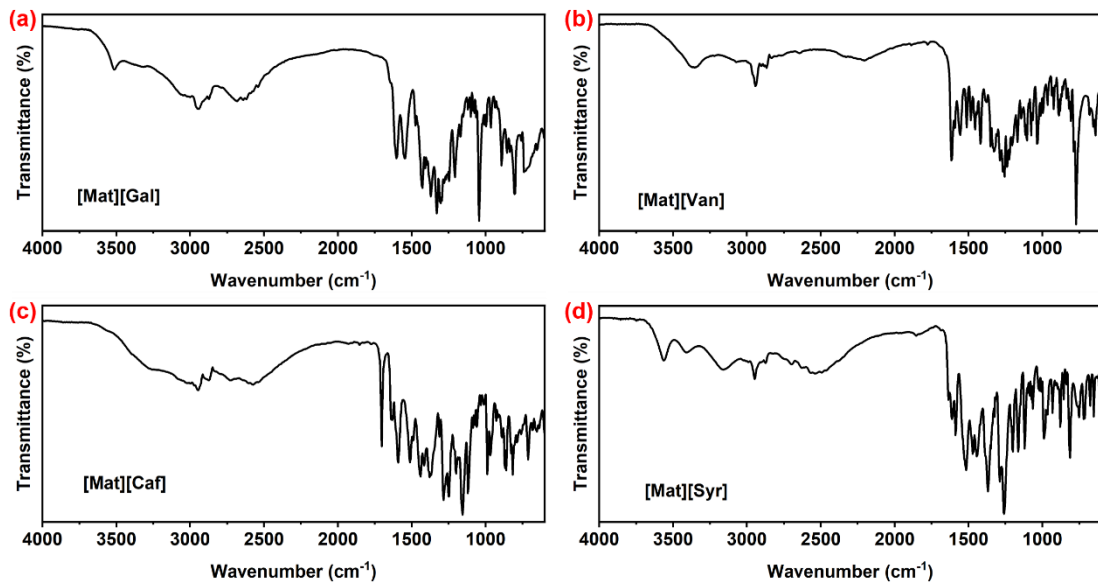


**Fig.2** FT-IR spectra of the matrinium-based supra-molecular ionic salts: (a) [Mat][Gal]; (b) [Mat][Van]; (c) [Mat][Caf]; (d) [Mat][Syr].

Furthermore, the single-crystal data of MSIS (Fig.3) confirmed the proton transfer between matrine and phenolic acids in MSIS. Results show that the 4 MSIS are all of the orthorhombic crystal structures with P2<sub>1</sub>2<sub>1</sub>2<sub>1</sub> space group and Z=4. For [Mat][Gal], [Mat][Van] and [Mat][Syr], there are 1, 2, 2 formula moieties along a-, b-, c- axis, respectively; while, for [Mat][Caf], there are 1, 1, 4 formula moieties along a-, b-, c- axis, respectively. The supra-molecular crystal stacking comes from the strong electrostatic interactions between the matrinium cations and phenolic anions and other weak interactions, especially the abundant intermolecular hydrogen bonds. There are mainly N2-H2···O5, C22-H22B···O5, C9-H9B···O1, O2-H2A···O4, C16-H16A···O3, and O1-H1···O4 in [Mat][Gal];

C21-H21B···O5, O6-H6B···O4, C8-H8A···O5, C17-H17A···O3, and O6-H6A···O5 in [Mat][Van]·H<sub>2</sub>O; C21-H21A···O4, N2-H2···O4, C14-H14···O4, C13-H13B···O6, C19-H19···O1, C16-H16A···O6, O6-H6B···O2, C24-H24A···O6, and O2-H2A···O3 in [Mat][Caf]·H<sub>2</sub>O; C9-H9B···O6, N2-H2···O2, C12-H12A···O1, C14-H14···O2, C22-H22B···O7, C24-H24A···O7, and C24-H24B···O1 in [Mat][Syr]·CH<sub>3</sub>OH. The hydrogen bonds form a complex network among the molecules to stabilize the supra-molecular crystal stacking.

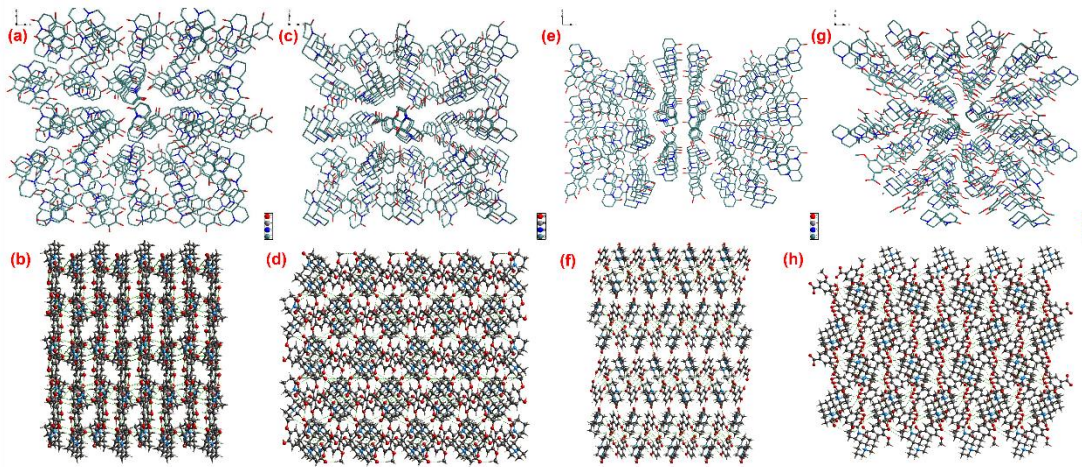


**Fig.3** Crystal stacking of the matrinium-based supra-molecular ionic salts: [Mat][Gal] viewing from a-axis (a) and b-axis with hydrogen bonds (b); [Mat][Van] viewing from a-axis (c) and c-axis with hydrogen bonds (d); [Mat][Caf] viewing from a-axis (e) and b-axis with hydrogen bonds (f); [Mat][Syr] viewing from a-axis (g) and b-axis with hydrogen bonds (h).

Element analysis of [Mat][Gal], [Mat][Van], [Mat][Caf] and [Mat][Syr] were conducted to investigate the purity of products. As is shown in Fig.4a, the consistency between the calculated and experimental results indicates the high purity of MSIS. Moreover, all the MSIS possess much higher water solubilities than that of their respective phenolic acids (Fig.4b). The water solubilities of [Mat][Gal], [Mat][Van], [Mat][Caf] and [Mat][Syr] were about 4, 668, 11, 556 folds of those of H[Gal], H[Van], H[Caf] and H[Syr], which is a significant benefit for improving bioavailability. The poor water solubilities of H[Van], H[Caf] and H[Syr] (0.78 – 1.87 mg/ml) can be attributed to their strong hydrogen interactions intra molecules, which have been presented in FT-IR spectra. The increase of water solubility after salt formation is probably induced by the complex intermolecular hydrogen interactions

(Fig.3), which decrease the intramolecular hydrogen bonds and offer more opportunities to form hydrogen bonding with water [20]. Due to the large difference among the water solubilities, the antibacterial assay was conducted at different concentration ranges, such as 0.125 – 32 mg/ml for [Mat][Gal], [Mat][Van], [Mat][Syr], and 0.125 – 8 mg/ml for H[Gal], [Mat][Caf]. Unfortunately, the MICs of H[Van], H[Caf], and H[Syr] are higher than their water solubilities. As is shown in Fig.4c, all the tested samples demonstrate a higher MIC against *E. coli* than that against *S. aureus*, which is probably attributed to the extra outer membrane of the gram-negative bacteria [21]. The antibacterial ability against *E. coli* decreases in an order of H[Gal] > [Mat][Gal] > [Mat][Caf] > [Mat][Van] > [Mat][Syr], while follows an order of H[Gal] > [Mat][Gal] > [Mat][Van] > [Mat][Caf] > [Mat][Syr] against *S. aureus*. Although H[Gal] features a significantly smaller MIC ( $p < 0.05$ ) against *E. coli* than those of all the MSIS, its MIC against *S. aureus* is much similar ( $p > 0.05$ ) to those of [Mat][Gal] and [Mat][Van]. Moreover, [Mat][Gal] and [Mat][Van] are 3 – 5 times their *S. aureus* MICs, indicating an excellent antibacterial selectivity, which is better than that of H[Gal]. Besides, the MICs against *E. coli* and *S. aureus* are 63.75 and 60.4 mm, respectively [13]. All the MSIS exhibit a much better antibacterial selectivity than that of matrine, for both *E. coli* and *S. aureus*.

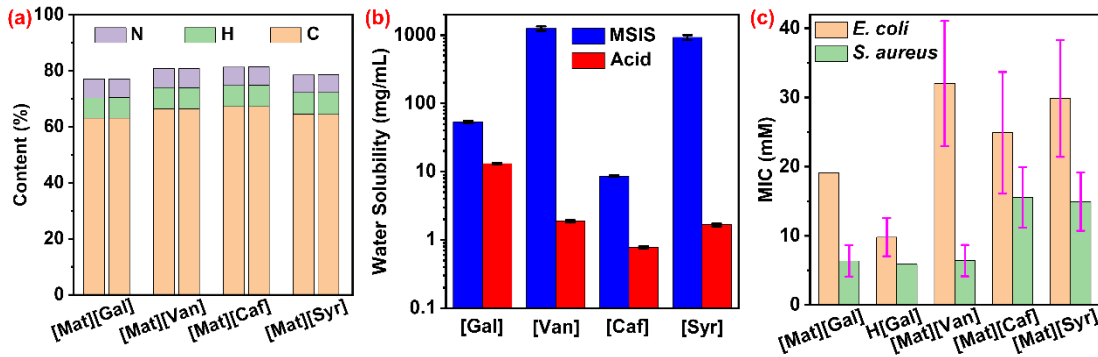


**Fig.4** (a) Calculated (left) and experiment (right) results for the element analysis of MSIS; Water solubility (b) and MIC (c) of MSIS and their respective phenolic acids.

The scavenging ability of free radicals is an important indicator of antioxidant performance. The DPPH radical scavenging results in Fig.5 show that all the MSIS feature lower IC<sub>50</sub> than those of their respective phenolic acids. The DPPH IC<sub>50</sub> values of MSIS decreases in the order of [Mat][Van] > [Mat][Syr] > [Mat][Caf] > [Mat][Gal], which is same

to that of their respective phenolic acids. The experiments indicate that the DPPH radical scavenging ability of matrine is poor, which is lower than 50% at the concentration of 1mg/ml (4026.25  $\mu$ M). Thus, it can be concluded that the phenolic anions play a key role in the antioxidant ability of MSIS. It is worth noting that salt formation with matrine has a greater impact on the antioxidant properties of phenolic acids with higher IC<sub>50</sub> values. The DPPH IC<sub>50</sub> value of [Mat][Van] is just 17.68% of that of H[Van]. Besides, the DPPH IC<sub>50</sub> values of all the MSIS are lower than that of AA (36.86  $\mu$ M, from experiments), indicating excellent antioxidant ability. The ABTS radical scavenging results in Fig.6 show that all the MSIS feature lower IC<sub>50</sub> than those of their respective phenolic acids. The ABTS IC<sub>50</sub> values of MSIS decreases in the order of [Mat][Van] > [Mat][Caf]  $\approx$  [Mat][Syr] > [Mat][Gal], which is same to that of their respective phenolic acids. The scavenging ability of matrine is also poor for ABTS radicals, without IC<sub>50</sub> until the concentration of 1mg/ml (4026.25  $\mu$ M). Thus, it further proves that the phenolic anions play a key role in the antioxidant ability of MSIS. Meanwhile, the salt formation with matrine also has the greatest impact on the antioxidant properties of H[Van], whose IC<sub>50</sub> value is 12.47 folds of that of [Mat][Van]. Besides, [Mat][Gal] has the strongest scavenging ability for both DPPH and ABTS radicals, with IC<sub>50</sub> values of 28.88% of AA and 29.45% of Trolox, indicating great potential application in commercial antioxidants.

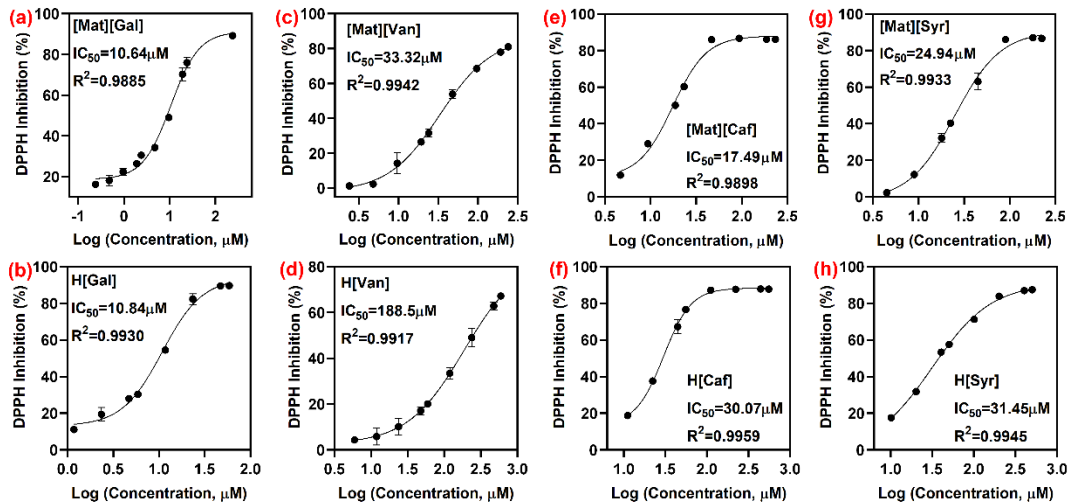


**Fig.5** DPPH radical scavenging results of (a) [Mat][Gal], (b) H[Gal], (c) [Mat][Van], (d) H[Van], (e) [Mat][Caf], (f) H[Caf], (g) [Mat][Syr] and (h) H[Syr].

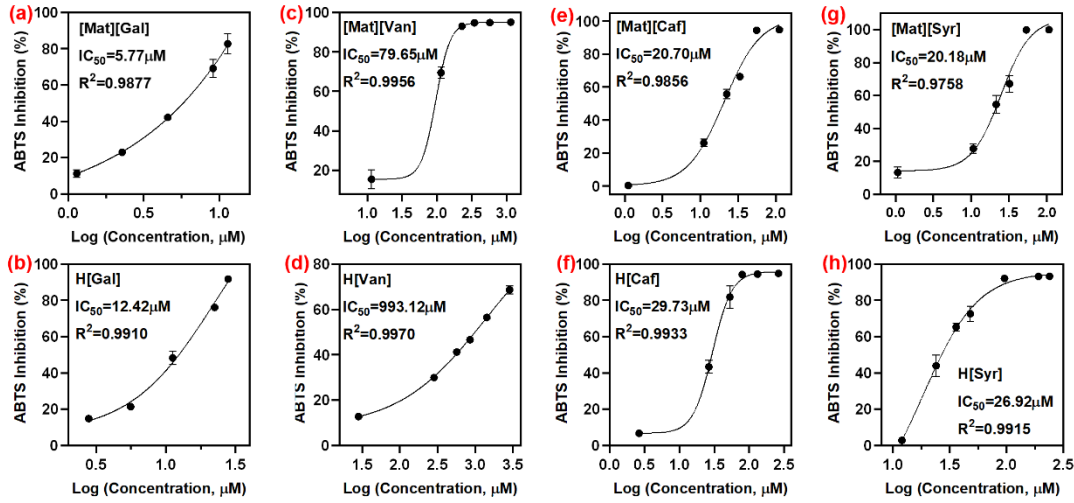


**Fig.6** ABTS radical scavenging results of (a) [Mat][Gal], (b) H[Gal], (c) [Mat][Van], (d) H[Van], (e) [Mat][Caf], (f) H[Caf], (g) [Mat][Syr] and (h) H[Syr].

Higher water solubility may lead to stronger toxicity. Thus, the cytotoxicity of matrine, phenolic acids, and MSIS were measured using NHEK cells. Results show that all the samples reduced the viability of NHEK cells in a dose-dependent manner (Fig.7a-d, f). All the MSIS feature higher cytotoxicity IC<sub>50</sub> values than those of their respective phenolic acids (Fig.7e). Although the cytotoxicity IC<sub>50</sub> values of MSIS follow the same trend as their respective phenolic acids, it is worth noting that when the IC<sub>50</sub> value of the phenolic acid is lower/higher than that of matrine, its MSIS also exhibits an IC<sub>50</sub> value lower/higher than that of matrine. This indicates that the cytotoxicity of MSIS is influenced by both phenolic anions and matrinium cations. For the phenolic acids with comparatively higher cytotoxicity, the IC<sub>50</sub> values increased sharply after salt formation with matrine. The IC<sub>50</sub> values of [Mat][Gal] and [Mat][Caf] are 4.17 and 3.35 folds of those of H[Gal] and H[Caf], respectively.

## Conclusion

4 MSIS, i.e. [Mat][Gal], [Mat][Van], [Mat][Caf], [Mat][Syr], were synthesized in this work. The NMR and FT-IR results indicate that the formation of MSIS is an atom-economic process between the phenolic acids and matrine, and the elemental analysis confirms the high purity of products. The single-crystal data demonstrate that the 4 MSIS are crystallized in the orthorhombic space group P2<sub>1</sub>2<sub>1</sub>2<sub>1</sub>, with abundant hydrogen-bonding interactions. With a synergistic effect between the matrine cations and phenolic anions, all the MSIS exhibit

enhanced water solubility, antibacterial activity, antioxidant efficiency, and lower cytotoxicity than those of their respective phenolic acids and matrine. The water solubilities of MSIS are 4 – 668 folds of their phenolic acids, while the MICs of MSIS are much lower than that of matrine, for both *E. coli* and *S. aureus*. Moreover, the DPPH and ABTS IC<sub>50</sub> values of MSIS are smaller than their respective phenolic acids and matrine, and the cytotoxicity IC<sub>50</sub> values of MSIS are higher than those of their respective phenolic acids. Thus, it can be concluded that salt formation with matrine is a feasible and effective strategy to increase the water solubility and bioactivity of phenolic acids.

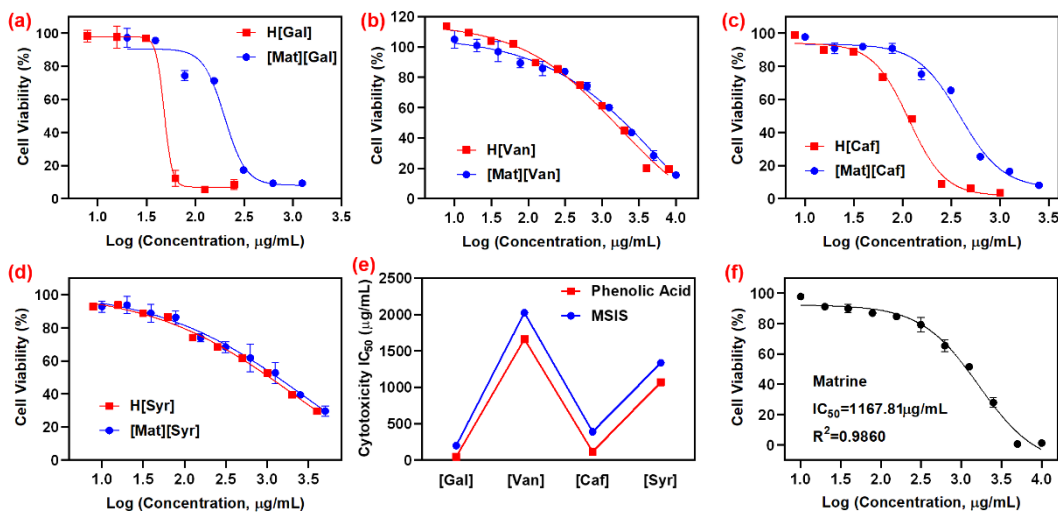


**Fig.7** Effect of MSIS and their respective phenolic acids on the viability of NHEK cells: (a) [Mat][Gal] and H[Gal], (b) [Mat][Van] and H[Van], (c) [Mat][Caf] and H[Caf], (d) [Mat][Syr] and H[Syr]; (e) Cytotoxicity IC<sub>50</sub> values of MSIS and their respective phenolic acids; (f) Effect of matrine on the viability of NHEK cells.

### Acknowledgments

This work was financially supported by the National Natural Science Foundation of China (Grant No. 21905069), the Shenzhen Science and Technology Innovation Committee (Grant Nos. JCYJ20180507183907224, KQTD20170809110344233, GXWD20201230155427003-20200821181245001), the Economic, Trade, and Information Commission of Shenzhen Municipality through the Graphene Manufacture Innovation Center (Grant No. 201901161514), the Guangdong Province Covid-19 Pandemic Control Research Fund

(2020KZDZX1220) and the Department of Science and Technology of Guangdong Province (Grant Nos. 2019A1515110754, 2020A1515110879).

### **Conflict of Interest Statement**

The authors declare no conflicts of interest.

### **References**

1. Ahmad NA, Jumbri K, et al (2019) Synthesis, characterisation and antioxidant properties of ferulate-based protic ionic liquids: Experimental and modelling approaches. *Journal of Molecular Liquids* 278: 309-319.
2. Aitipamula S and Das S (2020) Cocrystal formulations: A case study of topical formulations consisting of ferulic acid cocrystals. *Eur J Pharm Biopharm* 149: 95-104.
3. Alvarez-Lorenzo C, Castiñeiras A, et al (2020) Recurrent motifs in pharmaceutical cocrystals involving glycolic acid: X-ray characterization, Hirshfeld surface analysis and DFT calculations. *CrystEngComm* 22(40): 6674-6689.
4. Boyd BJ, Bergstrom CAS, et al (2019) Successful oral delivery of poorly water-soluble drugs both depends on the intraluminal behavior of drugs and of appropriate advanced drug delivery systems. *Eur J Pharm Sci* 137: 104967.
5. Chen X, Li D, et al (2021) Sinomenine-phenolic acid coamorphous drug systems: Solubilization, sustained release, and improved physical stability. *International Journal of Pharmaceutics* 598.
6. Cvetanovic A, Zengin G, et al (2018) Comparative in vitro studies of the biological potential and chemical composition of stems, leaves and berries Aronia melanocarpa's extracts obtained by subcritical water extraction. *Food Chem Toxicol* 121: 458-466.
7. Elfalleh W, Nasri N, et al (2009) Physico-chemical properties and DPPH-ABTS scavenging activity of some local pomegranate (*Punica granatum*) ecotypes. *Int J Food Sci Nutr* 60: 197-210.
8. Elsayed Azab A, A Adwas A, et al (2019) Oxidative stress and antioxidant mechanisms in human body. *Journal of Applied Biotechnology & Bioengineering* 6(1): 43-47.
9. Furia E, Beneduci A, et al (2021) Modeling the Solubility of Phenolic Acids in Aqueous Media at 37 degrees C. *Molecules* 26(21): 6500.

10. Gupta D, Bhatia D, et al (2018) Salts of Therapeutic Agents: Chemical, Physicochemical, and Biological Considerations. *Molecules* 23(7): 1719.
11. Hallan S, Sguizzato M, et al (2021) The Potential of Caffeic Acid Lipid Nanoparticulate Systems for Skin Application: In Vitro Assays to Assess Delivery and Antioxidant Effect. *Nanomaterials* 11(1).
12. Hu S, Wang C, et al (2020) Reducing the Sublimation Tendency of Ligustrazine through Salt Formation. *Crystal Growth & Design* 20(3): 2057-2063.
13. Kumar N and Goel N (2019) Phenolic acids: Natural versatile molecules with promising therapeutic applications. *Biotechnol Rep (Amst)* 24: e00370.
14. Li X, Liu X, et al (2021) Drug–Drug Cocrystallization Simultaneously Improves Pharmaceutical Properties of Genistein and Ligustrazine. *Crystal Growth & Design* 21(6): 3461-3468.
15. Moshikur RM, Chowdhury MR, et al (2018) Characterization and cytotoxicity evaluation of biocompatible amino acid esters used to convert salicylic acid into ionic liquids. *International Journal of Pharmaceutics* 546(1-2): 31-38.
16. Park JH, Lee M, et al (2014) Antioxidant activity of orange flesh and peel extracted with various solvents. *Prev Nutr Food Sci* 19(4): 291-298.
17. Paulo F and Santos L (2018) Microencapsulation of caffeic acid and its release using a w/o/w double emulsion method: Assessment of formulation parameters. *Drying Technology* 37(8): 950-961.
18. Ramli M, Hussein MZ, et al (2013) Preparation and characterization of an anti-inflammatory agent based on a zinc-layered hydroxide-salicylate nanohybrid and its effect on viability of Vero-3 cells. *Int J Nanomedicine* 8: 297-306.
19. Sintra TE, Luis A, et al (2015) Enhancing the antioxidant characteristics of phenolic acids by their conversion into cholinium salts. *ACS Sustain Chem Eng* 3(10): 2558-2565.
20. Wang Z, Zhang J, et al (2019) Novel bio-renewable matrinium-based ionic liquids derived from Chinese herb medicine: Synthesis, physicochemical properties and biological activity. *Journal of Molecular Liquids* 296: 111822.
21. Xie AG, Cai X, et al (2011) Long-acting antibacterial activity of quaternary phosphonium salts functionalized few-layered graphite. *Materials Science and Engineering: B* 176(15): 1222-1226.

22. Xing M, Yang G, et al (2021) Acid-base combination principles for preparation of anti-acne dissolving microneedles loaded with azelaic acid and matrine. *Eur J Pharm Sci* 165: 105935.
23. Yu Y and Liang G (2022) Interaction mechanism of phenolic acids and zein: A spectrofluorometric and molecular dynamics investigation. *Journal of Molecular Liquids* 348: 118032.
24. Zhang H, Chen L, et al (2020) Matrine: A Promising Natural Product With Various Pharmacological Activities. *Front Pharmacol* 11: 588.